Universal Tripartite Entanglement in One-Dimensional Many-Body Systems

Yijian Zou, 1,2,3 Karthik Siva, 4 Tomohiro Soejima, 4 Roger S. K. Mong, 5 and Michael P. Zaletel, 6

1 Perimeter Institute for Theoretical Physics, Waterloo, Ontario N2L 2Y5, Canada

2 University of Waterloo, Waterloo, Ontario N2L 3G1, Canada

3 Sandbox, Alphabet, Mountain View, California 94043, USA

4 Department of Physics, University of California, Berkeley, California 94720, USA

5 Department of Physics and Astronomy, University of Pittsburgh, Pittsburgh, Pennsylvania 15260, USA

6 Materials Sciences Division, Lawrence Berkeley National Laboratory, Berkeley, California 94720, USA

(Received 5 January 2021; accepted 26 February 2021; published 22 March 2021)

Motivated by conjectures in holography relating the entanglement of purification and reflected entropy to the entanglement wedge cross section, we introduce two related non-negative measures of tripartite entanglement g and h. We prove structure theorems which show that states with nonzero g or h have nontrivial tripartite entanglement. We then establish that in one dimension these tripartite entanglement measures are universal quantities that depend only on the emergent low-energy theory. For a gapped system, we argue that either $g \neq 0$ and h = 0 or g = h = 0, depending on whether the ground state has long-range order. For a critical system, we develop a numerical algorithm for computing g and h from a lattice model. We compute g and h for various CFTs and show that h depends only on the central charge whereas g depends on the whole operator content.

DOI: 10.1103/PhysRevLett.126.120501

Quantum entanglement has come to play a key role in our understanding of emergent phenomena in quantum many-body physics and modern numerical methods. Most attention has focused on bipartite entanglement, e.g., properties of a pure state on two parties $|\psi\rangle_{AB}$. The entanglement entropy S(A) is the unique measure of bipartite entanglement because, up to reversible local operations and classical communication, the EPR pair is the unique form of bipartite entanglement. In contrast, a pure tripartite state $|\psi\rangle_{ABC}$ admits a large (presumably infinite) number of distinct forms of entanglement, and, consequently, a variety of tripartite entanglement measures have been proposed [1]. But it remains relatively unexplored what universal features such measures might reveal about a many-body system [2–9].

Recently two tripartite entanglement measures, the entanglement of purification $E_P(A:B)$ [10] and the reflected entropy $S_R(A:B)$ [11] have been applied to many-body physics within the context of holographic duality. As motivation, recall that the Ryu-Takayanagi formula equates the bipartite entanglement entropy of a boundary theory to the area of a minimal surface in its holographic dual [12], a central result in the effort to relate the emergence of spacetime geometry to quantum entanglement. It is then natural ask whether there are multipartite entanglement measures which might also have a dual geometric interpretation. In Refs. [13,14] it was conjectured that the minimal cross section of the bulk entanglement wedge joining two parties, $E_W(A:B)$, is dual to the entanglement of purification in the boundary, $E_P = E_W$.

More recently, however, by developing a field-theoretic method for calculating S_R in generic conformal field theories (CFTs), it was shown that $S_R = 2E_W$ [11]. In general, $S_R \neq 2E_P$, so one possible resolution is that their equality is a special property of holographic CFTs which is violated at subleading order in large-N expansion [15]. The gap between them, $2E_P - S_R$, would then constitute an interesting entanglement measure of this violation. But investigating this discrepancy requires a method for computing these quantities in generic many-body systems.

In this work we derive a method for computing E_P and S_R in 1D lattice models. To summarize our findings it is convenient to define UV-regularized version of these quantities [16], $g(A:B) \equiv 2E_P(A:B) - I(A:B) \ge 0$ and $h(A:B) \equiv S_R(A:B) - I(A:B) \ge 0$, where I is the mutual information [17]. For the tripartition of a ring shown in Fig. 1, holographic duality predicts that they take on the universal value $g = h = (c/3)\log(2)$, where c is the

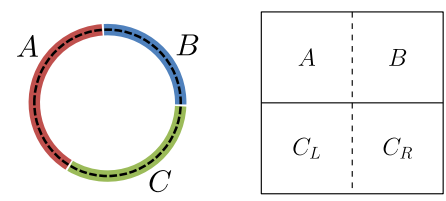


FIG. 1. Left: A spin chain on a circle that is divided into three parties A, B, and C. Right: Geometry in the computation of $E_P(A:B)$. Region C is divided into C_L and C_R . The dashed line represents the entanglement cut between AC_L and BC_R .

central charge of the CFT [18]. But what about in a generic lattice model? As a limiting case, we start by proving structure theorems for states with g, h = 0 which imply that h = 0 if an only if a state is gapped (c = 0), while g = 0 if and only if the system is gapped and does not spontaneously break a symmetry. We then develop a method for numerically computing g, h from a lattice Hamiltonian on systems up to $N \sim 100$ sites. As expected, we find that $h = (c/3) \log 2$ is universal. However we find that $g \ge h$ and depends on the operator content of the CFT in addition c, yet is nevertheless completely universal. Thus, $2E_P - S_R = g - h$ constitutes a new and universal tripartite entanglement invariant of CFTs.

 E_P and S_R .—We first review the definitions of the entanglement of purification $E_P(A:B)$ and reflected entropy $S_R(A:B)$. Unlike the bipartite entanglement entropy, which is a function of a reduced density matrix on one party, these mixed state entanglement measures are functions of the reduced density matrix on two parties, ρ_{AB} , or equivalently its purification $|\psi\rangle_{ABC}$, where $\rho_{AB} = \mathrm{Tr}_C |\psi\rangle\langle\psi|$.

The entanglement of purification $E_P(A:B)$ [10] is the minimum of the entanglement entropy S_{AC_L} over all purifications $|\phi\rangle_{ABC_LC_R}$ of ρ_{AB} to another pair of systems $C = C_LC_R$:

$$E_P(A:B) \equiv \min_{|\phi\rangle} S_{AC_L}(|\phi\rangle_{ABC_LC_R}). \tag{1}$$

The partitions of the subsystems are depicted schematically in Fig. 1. In principle the auxiliary space $C_L C_R$ can be arbitrary, but the minimal S_{AC_L} can always be achieved with $\dim(\mathcal{H}_{C_L}), \dim(\mathcal{H}_{C_R}) \leq \operatorname{rank}(\rho_{AB})$ [19]. We may alternatively rephrase Eq. (1) as a minimization over unitary operations U_C restricted to $C_L C_R$ starting from an *arbitrary* purification $|\phi_0\rangle_{ABC_L C_R}$ of sufficiently large dimension,

$$E_P(A:B) = \min_{U_{C_L C_R}} S_{AC_L}(U_C | \phi_0 \rangle_{ABC_L C_R}), \qquad (2)$$

which is the viewpoint taken in our numerical approach. E_P is lower bounded by the mutual information [10], $E_P(A:B) \ge I(A:B)/2$, so we define a non-negative quantity

$$g(A:B) \equiv 2E_P(A:B) - I(A:B) \ge 0.$$
 (3)

The physical intuition behind this new quantity is that the subtraction of the mutual information removes correlations which are purely bipartite, as will be made more precise by the structure theorems below.

To define the reflected entropy $S_R(A:B)$, we instead pick a particular purification of ρ_{AB} known as the canonical purification $|\sqrt{\rho_{AB}}\rangle$. It is defined as follows: we first take the unique non-negative square root of the reduced density matrix ρ_{AB} , and then regard the operator $\sqrt{\rho_{AB}}$ as a state

 $|\sqrt{\rho_{AB}}\rangle \in \mathcal{H}_A \otimes \mathcal{H}_B \otimes \mathcal{H}_A^* \otimes \mathcal{H}_B^*$. The reflected entropy $S_R(A:B)$ is defined as

$$S_R(A:B) \equiv S_{AA^*}(|\sqrt{\rho_{AB}}\rangle).$$
 (4)

It is shown in Ref. [11] that $S_R(A:B) \ge I(A:B)$, so we define the nonnegative quantity

$$h(A:B) \equiv S_R(A:B) - I(A:B) \ge 0. \tag{5}$$

In order to interpret the nature of the tripartite entanglement captured by these quantities, we derive "structure theorems" for states that saturate these lower bounds, i.e., states with g=0 or h=0.

States with g(A: B) = 0.—We first define a class of pure tripartite wave functions known as *triangle states*.

Definition 1.—[Triangle State] A state $|\psi\rangle_{ABC}$ is a triangle state if for each local Hilbert space there exists a bipartition $\mathcal{H}_{\alpha}=\mathcal{H}_{\alpha_L}\otimes\mathcal{H}_{\alpha_R}$ ($\alpha=A,\,B,\,C$) such that

$$|\psi\rangle_{ABC} = |\psi\rangle_{A_RB_L}|\psi\rangle_{B_RC_L}|\psi\rangle_{C_RA_L},\tag{6}$$

where $|\psi\rangle_{\alpha_R\beta_L}$ are pure states in $\mathcal{H}_{\alpha_R}\otimes\mathcal{H}_{\beta_L}$.

In other words, a triangle state can be obtained by pairwise distributing bipartite-entangled states followed by local unitaries. In this sense, a triangle state lacks nontrivial tripartite entanglement. We prove the following theorem in the Supplemental Material [20,21].

Theorem 2.—A state $|\psi\rangle_{ABC}$ is a triangle state up to local isometries if and only if g(A:B) = 0.

The "only if" direction can be shown by noting that $2E_P(A:B) = I(A:B)$ in the purification $|\psi\rangle_{ABC}$ of ρ_{AB} . The proof of the "if" direction is more complicated, and is presented in the Supplemental Material [20].

Conversely, g(A:B) > 0 implies that $|\psi\rangle_{ABC}$ contains tripartite entanglement that cannot be factorized pairwise. For example, for a GHZ state $|\psi\rangle_{ABC} = \sqrt{d^{-1}\sum_{j=1}^{d}|j_Aj_Bj_C\rangle}$ the optimal purification of ρ_{AB} is $|\psi\rangle_{ABC}$ itself [14], resulting in $g(A:B) = \log d$. It can also be shown that the W state has nonzero g(A:B). This is in accordance with the fact the GHZ state and W state are not triangle states [22].

States with h(A:B) = 0.—It can be verified that a triangle state has h(A:B) = 0, so $h(A:B) \neq 0$ also implies irreducible tripartite entanglement. But for the GHZ state, $g(A:B) \neq 0$ while h(A:B) = 0, which suggests that some forms of tripartite entanglement are "invisible" to h.

To make this precise we introduce the notion of the sum of triangle states.

Definition 3.—A pure state $|\psi\rangle_{ABC}$ is a SOTS if for each local Hilbert space \mathcal{H}_{α} there exists a decomposition $\mathcal{H}_{\alpha} = \bigoplus_{j} \mathcal{H}_{\alpha_{L}^{j}} \otimes \mathcal{H}_{\alpha_{R}^{j}}$, such that

$$|\psi\rangle_{ABC} = \sum_{j} \sqrt{p_{j}} |\psi_{j}\rangle_{A_{R}^{j}B_{L}^{j}} |\psi_{j}\rangle_{B_{R}^{j}C_{L}^{j}} |\psi_{j}\rangle_{C_{R}^{j}A_{L}^{j}}, \quad (7)$$

where $|\psi_j\rangle_{\alpha_R^j\beta_L^j}$ represents a pure state in $\mathcal{H}_{\alpha_R^j}\otimes\mathcal{H}_{\beta_L^j}$, etc., and $\sum_j p_j=1$.

For example, the GHZ state is a SOTS with $p_j = 1/d$ and the triangle state is a SOTS for which $p_j = 1$ for exactly one j. By using the structure theorem for states satisfying strong subadditivity [23], we prove [20] the following:

Theorem 4.—A state $|\psi\rangle_{ABC}$ is a SOTS if and only if h(A:B)=0.

As a corollary, while in general $h(A:B) \neq h(B:C) \neq h(C:A)$, if one vanishes then all of them vanish (and likewise for q).

g and h for 1D gapped systems.—We now give a physical interpretation of these structure theorems in the context of 1D Hamiltonians: we argue that on a ring with the tripartition shown in Fig. 1, a system is gapped if and only if h = 0, and gapped without long-range order if and only if g = 0. As motivation, consider the two limiting gapped phases of the 1D Ising model: the symmetric paramagnet, $|PM\rangle = | \rightarrow \rightarrow \cdots \rangle$, and the ferromagnet $|FM\rangle = (1/\sqrt{2})(|\uparrow\uparrow\cdots\rangle + |\downarrow\downarrow\cdots\rangle)$. When partitioned into 3 subsystems, the |PM\rangle (|FM\rangle) state corresponds to a product state (GHZ state), so it will have q = 0 $(g = \log 2)$ and for both h = 0. Indeed, we see that g is sensitive to the "cat state" structure of the exact ground state in a symmetry-broken phase, so will generically detect the multiplicity of superselection sectors. Away from these extremal points, the ground state develops additional shortrange entanglement. However, so long as sizes of the regions N_A , N_B , N_C are larger than the correlation length ξ , this additional entanglement simply dresses the product state within each superselection sector into a triangle state, and so with exponential accuracy in N/ξ , g and h are unchanged.

The argument can be phrased most precisely in the language of matrix product states. We first take a finitedimensional MPS as an approximation to the ground state of a 1D system [24]. The thermodynamic limit is taken by fixing N_A/N , N_B/N and taking $N \to \infty$, where N is the total system size. In the thermodynamic limit we can then apply the standard MPS coarse-graining procedure [29] to obtain a fixed-point MPS. If the initial correlation length is finite [30], the state flows to an MPS with $\xi = 0$. It is straightforward to show that a $\xi = 0$ MPS is precisely the N-party generalization [31] of a triangle state [29,32], so by the structure theorems we obtain g = h = 0. On the other hand, if the MPS has an infinite correlation length (e.g., it is a cat state as occurs for spontaneous symmetry breaking or phase coexistence), then it flows to a sum of $\xi = 0$ MPS which are locally orthogonal [20,28]. Thus in the longrange ordered phase we have $g \neq 0$ and h = 0. These cases are analyzed in greater detail in Ref. [20]. Note that the precise statement of our claim is thus as follows: A fixed-point MPS has h(A:B)=0 for all contiguous tripartitions. Since all MPS flow towards fixed-point MPS under coarse graining, $h(A:B) \to 0$ as $N_A, N_B \to \infty$ [33].

Gapless systems.—At a critical point g and h need not vanish. In fact, they are universal constants which depend only on the emergent CFT in the thermodynamic limit.

We now briefly describe the algorithm to compute g and h of the ground state of a critical quantum spin chain with N sites and Hamiltonian H. First the ground state $|\psi\rangle_{ABC}$ is obtained in the form of a periodic uniform MPS (puMPS) [35–37]. A puMPS consists of N copies of the same rank-3 tensor M with dimensions $D \times D \times d$, where d is the dimension of the Hilbert space on each site, and D is the bond dimension which grows polynomially with the system size N (Fig. 2). The tensor M is obtained variationally by minimizing the expectation value of H. We then apply the standard MPS coarse-graining procedure [20,29] to "compress" the Hilbert space of each region down to a smaller one via a sequence of isometries, $\mathcal{H}_{\alpha} \to \mathcal{H}_{\tilde{\alpha}}$. Because the entropy of each region is subextensive, $S_{\alpha} \ll N_{\alpha} \log(d)$ —even at a critical point—we can reduce the dimension of the Hilbert space $\tilde{d}_{\alpha} \ll d_{\alpha}$ while preserving all the bipartite and tripartite entanglement properties among the three parties A, B, and C to high accuracy. The coarse-grained state $|\tilde{\psi}\rangle_{\tilde{A}\tilde{B}\tilde{C}}$ can be represented by a MPS with three tensors M_{α} with dimensions $D \times D \times \tilde{d}_{\alpha}$ (Fig. 2), where $\tilde{d}_{\alpha} \leq D^2$. D, \tilde{d}_{α} grow polynomial with system size; as an example, for the Ising CFT we use D=12, $\tilde{d}_{\alpha}=36$ for N=24 and D=26, $\tilde{d}_{\alpha}=100$ for N = 84.

We compute $S_R(A:B)$ according to Eq. (4) in the dense representation. Assuming that $\tilde{d}_A \leq \tilde{d}_B$, the total time cost scales as $\mathcal{O}(\tilde{d}_A^4 \tilde{d}_B^2)$. To compute $E_P(A:B)$, we first make a random split of $\mathcal{H}_{\tilde{C}}$ into $\mathcal{H}_{\tilde{C}_L} \otimes \mathcal{H}_{\tilde{C}_R}$ with dimensions $\tilde{d}_{C_L} \times \tilde{d}_{C_R}$. We then numerically minimize the entanglement entropy of $\tilde{A}\tilde{C}_L$ with respect to a unitary $U_{\tilde{C}}$ on \tilde{C} ,

$$E_P(A:B) = \min_{U_{\tilde{C}}} S_{\tilde{A}\tilde{C}_L}(U_{\tilde{C}}|\tilde{\psi}\rangle_{\tilde{A}\tilde{B}\tilde{C}}). \tag{8}$$

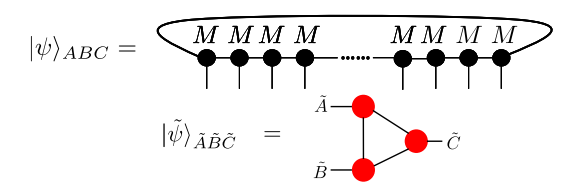


FIG. 2. The state before and after coarse-graining. Top: The periodic uniform matrix product state (puMPS) represents the ground state of a translation-invariant critical quantum spin chain before coarse-graining. Bottom: The puMPS is coarse-grained into a MPS with 3 tensors corresponding to the coarse-grained Hilbert spaces $\mathcal{H}_{\tilde{A}}$, $\mathcal{H}_{\tilde{B}}$, $\mathcal{H}_{\tilde{C}}$.

We verified numerically that the \tilde{d}_{α} are large enough to achieve the (near) optimal purification. The numerical optimization can be performed with, e.g., the nonlinear conjugate gradient algorithm, since the gradient can be constructed explicitly (see Ref. [20]). The time cost of each gradient calculation scales as $\mathcal{O}(\tilde{d}_A^2\tilde{d}_B\tilde{d}_C^2)$, assuming that $\tilde{d}_A \leq \tilde{d}_B$. The mutual information $I(A\colon B)$ can also be computed using the coarse-grained state, with time cost $O(\tilde{d}_{\max}^3)$, where $\tilde{d}_{\max} \equiv \max_{\alpha} \{\tilde{d}_{\alpha}\}$.

g and h for various CFTs.—In order to show that g and h are universal, we study the Ising model with an irrelevant near-to-nearest neighbor interaction [38],

$$H = \sum_{j=1}^{N} \begin{bmatrix} -X_{j}X_{j+1} - Z_{j} \\ +\lambda(X_{j}X_{j+1}Z_{j+2} + Z_{j}X_{j+1}X_{j+2}) \end{bmatrix}, \quad (9)$$

where $X_j(Z_j)$ are Pauli X(Z) matrices on sites j and periodic boundary conditions are assumed. The model is critical, described by the Ising CFT for $\lambda < \lambda^*$, gapped for $\lambda > \lambda^*$, where the transition at $\lambda^* \approx 0.428$ is described by the tricritical Ising CFT [38]. We study four parameter values, $\lambda = 0, 0.3, 0.4, \lambda^*$, where the first three correspond to the Ising CFT and the last corresponds to the tricritical Ising CFT.

We fix $N_A = N_B = N_C = N/3$ and compute g(A:B) and h(A:B) as a function of N, shown in Fig. 3. We see that both g and h converge to a constant as $N \to \infty$ [39]. Furthermore, the constant is the same for $\lambda = 0$ and $\lambda = 0.3$, indicating that g and h are universal. We denote the universal quantities as g^{CFT} and h^{CFT} . At $\lambda = \lambda^* \approx 0.428$, we obtain a different value that corresponds to the tricritical Ising CFT. At $\lambda = 0.4$, both g and h go through a renormalization group flow from the tricritical Ising CFT to the Ising CFT, analogous to the spectral flow observed in Ref. [35]. The values of g^{CFT} and h^{CFT} for various CFTs are summarized in Table I.

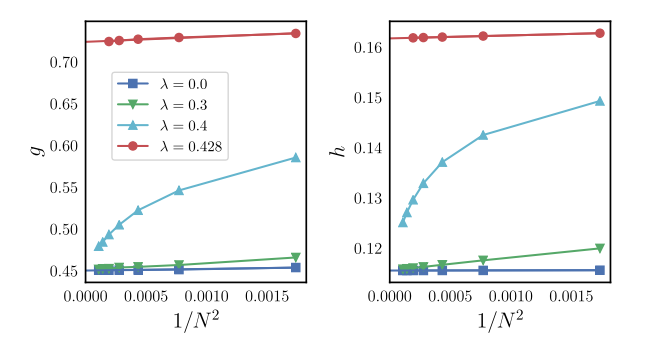


FIG. 3. g(A:B) and h(A:B) from the model Eq. (9) with different λ 's. At $\lambda=0$ and $\lambda=0.3$, the quantities converge to g^{CFT} and h^{CFT} of the Ising CFT. At $\lambda=\lambda^*\approx 0.428$, both quantities converge to a different value that corresponds to the tricritical Ising CFT. At $\lambda=0.4$ we observe a renormalization group flow from the tricritical Ising CFT to the Ising CFT.

TABLE I. g^{CFT} and h^{CFT} extracted numerically through finite size scaling. For the gapped spin chains, the universal values of g and h are shown. For the gapless spin chains, we show the central charge c as well as g^{CFT} and h^{CFT} of the CFTs.

Theory	С	g^{CFT}	h^{CFT}	$(c/3)\log 2$
Gapped symmetric	0	0	0	0
Long-range ordered	0	> 0	0	0
Ising CFT	1/2	0.450	0.1155	0.11553
Tricritical Ising CFT	7/10	0.719	0.1617	0.16173
Free boson $R = \sqrt{3}$	1	0.920	0.2310	0.23105
Free boson $R = 2$	1	0.899	0.2310	0.23105
Free boson $R = \sqrt{6}$	1	0.906	0.2310	0.23105

We also verified that the values of g^{CFT} and h^{CFT} do not depend on the relative sizes of A, B, C [20]. For any ratio N_A/N and N_B/N , once we take the thermodynamic limit $N \to \infty$, both g(A:B) and h(A:B) converge to the universal constants g^{CFT} and h^{CFT} .

We proceed to examine how g^{CFT} and h^{CFT} depend on the conformal data of the CFT. To do so we compute g^{CFT} and h^{CFT} for the free compactified boson CFT for differing compactification radius R. All have the same central charge c=1, but the operator content depends on R. A concrete lattice realization of the CFT is the XXZ model,

$$H = \sum_{j} (X_{j}X_{j+1} + Y_{j}Y_{j+1} + \Delta Z_{j}Z_{j+1}), \tag{10}$$

where $-1 \le \Delta < 1$ is a parameter that determines the compactification radius $R = \sqrt{2\pi/\cos^{-1}(-\Delta)}$. We compute g^{CFT} and h^{CFT} for different R's by extrapolating g(A:B) and h(A:B) for different Δ 's to the thermodynamic limit. The result is shown in Fig. 4 and Table I, where $R = \sqrt{3}$, 2, $\sqrt{6}$ correspond to $\Delta = 0.5$, 0, -0.5, respectively [40].

We see that h^{CFT} does not depend on Δ and is compatible with $h^{\text{CFT}} = (c/3) \log 2$. On the other hand, g^{CFT} depends on Δ and thus on R. For example, as shown in Table I, g^{CFT} takes on three different values at $\Delta = 0, 0.5, -0.5$, which correspond to $R = 2, \sqrt{3}, \sqrt{6}$, respectively. We conclude that h^{CFT} only depends on the central charge but g^{CFT} depends on the whole operator content. This feature of h^{CFT} can be understood as follows. The canonical purification of ρ_{AB} can be regarded as the ground state of a CFT living on a circle, divided into four contiguous segments A, B, \bar{B} , \bar{A} . The measure $h(A:B) = S_{A\bar{A}} - S_A - S_B + S_{AB}$ involves only contiguous pieces and is hence proportional to the central charge.

Discussion.—In this work we have introduced two positive quantities g and h which quantify the obstruction to factorizing a tripartite state into pairwise correlations. While the entanglement wedge cross section duality $E_W = E_P = S_R/2$ predicts $h = g = (c/3) \log(2)$, for low-c CFTs

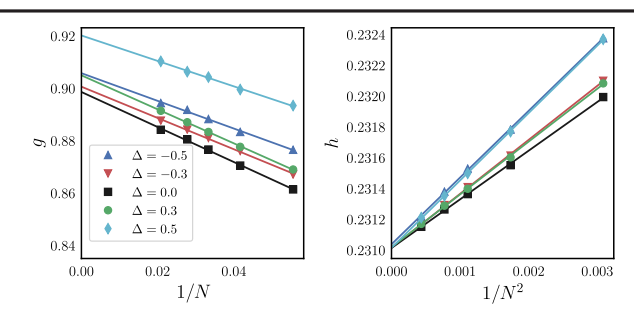


FIG. 4. g(A:B) and h(A:B) from the XXZ model with different Δ 's at sizes $18 \le N \le 48$. We see that g^{CFT} depends on Δ while h^{CFT} is independent of Δ .

like the Ising model we find $g > h = (c/3) \log(2)$. The gap g - h is universal, but it remains an open question how to compute it from the underlying data of the CFT. It is natural to conjecture a general bound $g \ge h$, which would follow from the monotonicity of S_R under a partial trace.

The authors are grateful to Ning Bao, Jeongwan Haah, and Guifre Vidal for enlightening conversations. We are particularly indebted to Brian Swingle both for our earlier collaborations and the suggestion to compute S_R . Y. Z. acknowledges Compute Canada. Research at Perimeter Institute is supported by the Government of Canada through the Department of Innovation, Science and Economic Development Canada and by the Province of Ontario through the Ministry of Research, Innovation and Science. Sandbox is a team within the Alphabet family of companies, which includes Google, Verily, Waymo, X, and others. K. S. acknowledges support from the NSF Graduate Research Fellowship Program (Grant No. DGE 1752814). R. M. is supported by the National Science Foundation under DMR-1848336. M. P. Z. was supported the DOE, Office of Science, Office of High Energy Physics under QuantISED Award No. DE-SC0019380 and under Contract No. DE-AC02-05CH11231.

- [1] M. Walter, D. Gross, and J. Eisert, Multipartite entanglement, in *Quantum Information: From Foundations to Quantum Technology Applications* (Wiley-VCH Verlag GmbH & Co. KGaA, Weinheim, 2016), p. 293, https://doi.org/10.1002/9783527805785.ch14.
- [2] K. Audenaert, J. Eisert, M. B. Plenio, and R. F. Werner, Entanglement properties of the harmonic chain, Phys. Rev. A 66, 042327 (2002).
- [3] S. Marcovitch, A. Retzker, M. B. Plenio, and B. Reznik, Critical and noncritical long-range entanglement in Klein-Gordon fields, Phys. Rev. A 80, 012325 (2009).
- [4] A. Bayat, P. Sodano, and S. Bose, Negativity as the entanglement measure to probe the kondo regime in the spin-chain kondo model, Phys. Rev. B 81, 064429 (2010).
- [5] A. Bhattacharyya, A. Jahn, T. Takayanagi, and K. Umemoto, Entanglement of Purification in Many Body

- Systems And Symmetry Breaking, Phys. Rev. Lett. 122, 201601 (2019).
- [6] J. Kudler-Flam and S. Ryu, Entanglement negativity and minimal entanglement wedge cross sections in holographic theories, Phys. Rev. D 99, 106014 (2019).
- [7] Y. Kusuki, J. Kudler-Flam, and S. Ryu, Derivation of Holographic Negativity in ads₃/cft₂, Phys. Rev. Lett. 123, 131603 (2019).
- [8] A. Bayat, Scaling of Tripartite Entanglement at Impurity Quantum Phase Transitions, Phys. Rev. Lett. 118, 036102 (2017).
- [9] J. Gray, A. Bayat, A. Pal, and S. Bose, Scale invariant entanglement negativity at the many-body localization transition, arXiv:1908.02761.
- [10] B. M. Terhal, M. Horodecki, D. W. Leung, and D. P. DiVincenzo, The entanglement of purification, J. Math. Phys. (N.Y.) 43, 4286 (2002).
- [11] S. Dutta and T. Faulkner, A canonical purification for the entanglement wedge cross-section, arXiv:1905.00577 (to be published).
- [12] S. Ryu and T. Takayanagi, Holographic Derivation of Entanglement Entropy from the Anti-de Sitter Space/Conformal Field Theory Correspondence, Phys. Rev. Lett. 96, 181602 (2006).
- [13] K. Umemoto and T. Takayanagi, Entanglement of purification through holographic duality, Nat. Phys. 14, 573 (2018).
- [14] P. Nguyen, T. Devakul, M. G. Halbasch, M. P. Zaletel, and B. Swingle, Entanglement of purification: From spin chains to holography, J. High Energy Phys. 01 (2018) 098.
- [15] It has also been argued that the logarithmic negativity is dual to E_W [7], but \mathcal{E}_N is not lower bounded by I, so we do not consider it here.
- [16] $2E_P(A:B)$, $S_R(A:B)$ and I(A:B) all scale logarithmically with the UV cutoff with the same coefficient c/3 in front, see Refs. [11,13], and [14].
- [17] Note that while the constituents are, *g*, *h* are not monotonic under quantum operations on *A*, *B*.
- [18] In this computation, the regions A, B are taken to touch and the UV divergences in E_W , I are regulated by a radial cutoff which is taken to zero after the subtraction $2E_W I$ [14]. This prescription corresponds to the lattice regularization employed in our numerical results. An alternative procedure, in which the quantities are regularized by a small spacing between A, B, yields a different result [13].
- [19] B. Ibinson, N. Linden, and A. Winter, Robustness of quantum Markov chains, Commun. Math. Phys. **277**, 289 (2007).
- [20] See Supplemental Material at http://link.aps.org/ supplemental/10.1103/PhysRevLett.126.120501 for proof of the structure theorems and numerical algorithms for gapless systems.
- [21] J. Haah (private communication).
- [22] W. Dür, G. Vidal, and J. I. Cirac, Three qubits can be entangled in two inequivalent ways, Phys. Rev. A 62, 062314 (2000).
- [23] P. Hayden, R. Jozsa, D. Petz, and A. Winter, Structure of states which satisfy strong subadditivity of quantum entropy with equality, Commun. Math. Phys. 246, 359 (2004).

- [24] There is a caveat to use the finite-dimensional MPS as an approximation. It is only rigorously proven that the state can be faithfully represented if bond dimension grows with the system size [25,26]. For a finite bond dimension, it has only been shown that local properties can be well approximated [27]. In order to make our argument, we have to assume that the finite bond dimension does not result in a substantial error in q or h, which are nonlocal properties of the ground state. Despite not rigorous proven, the assumption is highly plausible because of empirical success of infinite MPS algorithms, where correlation functions and entanglement properties at long distances are extracted from a finitedimensional MPS. Therefore the argument could be regarded as heuristic for a general gapped theory. However, it is rigorous if the ground state can be exactly represented by a finite-dimensional MPS, for example that of a MPS parent Hamiltonian [28].
- [25] F. Verstraete and J. I. Cirac, Matrix product states represent ground states faithfully, Phys. Rev. B 73, 094423 (2006).
- [26] I. Arad, A. Kitaev, Z. Landau, and U. Vazirani, An area law and sub-exponential algorithm for 1d systems, arXiv:1301.1162 (to be published).
- [27] A. M. Dalzell and F. G. S. L. Brandão, Locally accurate MPS approximations for ground states of one-dimensional gapped local Hamiltonians, Quantum 3, 187 (2019).
- [28] D. Perez-Garcia, F. Verstraete, M. M. Wolf, and J. I. Cirac, Matrix product state representations, Quantum Inf. Comput. 7, 401 (2007).
- [29] F. Verstraete, J. I. Cirac, J. I. Latorre, E. Rico, and M. M. Wolf, Renormalization-Group Transformations on Quantum States, Phys. Rev. Lett. 94, 140601 (2005).
- [30] M. B. Hastings and T. Koma, Spectral gap and exponential decay of correlations, Commun. Math. Phys. 265, 781 (2006).

- [31] The generalization of a triangle state to many parties is a polygon state, which is discussed in detail in Ref. [20]. A polygon state is a triangle state with respect to any tripartition into contiguous regions.
- [32] X. Chen, Z.-C. Gu, and X.-G. Wen, Classification of gapped symmetric phases in one-dimensional spin systems, Phys. Rev. B 83, 035107 (2011).
- [33] Technically, taking the limit assumes the continuity of g(A:B) and h(A:B) with respect to the reduced density matrix ρ_{AB} [20]. The continuity property of E_P and S_R has already been proven in Refs. [10,34].
- [34] C. Akers and P. Rath, Entanglement wedge cross sections require tripartite entanglement, J. High Energy Phys. 04 (2020) 208.
- [35] Y. Zou, A. Milsted, and G. Vidal, Conformal Data and Renormalization Group Flow in Critical Quantum Spin Chains Using Periodic Uniform Matrix Product States, Phys. Rev. Lett. **121**, 230402 (2018).
- [36] Y. Zou, A. Milsted, and G. Vidal, Conformal Fields and Operator Product Expansion in Critical Quantum Spin Chains, Phys. Rev. Lett. 124, 040604 (2020).
- [37] Y. Zou and G. Vidal, Emergence of conformal symmetry in quantum spin chains: Antiperiodic boundary conditions and supersymmetry, Phys. Rev. B 101, 045132 (2020).
- [38] E. O'Brien and P. Fendley, Lattice Supersymmetry and Order-Disorder Coexistence in the Tricritical Ising Model, Phys. Rev. Lett. 120, 206403 (2018).
- [39] The extrapolation is based on the numerical observation that g and h converges as a power of 1/N, where the power is determined empirically.
- [40] Note that at $\Delta = 0$ both g^{CFT} and h^{CFT} equal twice of that for the Ising CFT, in accordance with the duality between the CFTs.